# The effect of Mg doping on the structural and physical properties of $LuFe_2O_4$ and $Lu_2Fe_3O_7$



2009 J. Phys.: Condens. Matter 21 015401

(http://iopscience.iop.org/0953-8984/21/1/015401)

J. Phys.: Condens. Matter **21** (2009) 015401 (7pp) doi:10.1088/0953-8984/21/1/015401

# The effect of Mg doping on the structural and physical properties of $LuFe_2O_4$ and $Lu_2Fe_3O_7$

**Y B Qin[1], H X Yang[1,4], Y Zhang[1], H F Tian[2], C Ma[1], Y G Zhao[2], R I Walton[3] and J Q Li[1]**

[1] Beijing National Laboratory for Condensed Matter Physics, Institute of Physics, Chinese Academy of Sciences, Beijing 100190, People's Republic of China
[2] Department of Physics, Tsinghua University, Beijing 100084, People's Republic of China
[3] Department of Chemistry, University of Warwick, Coventry CV4 7AL, UK

Received 22 September 2008, in final form 28 October 2008
Published 1 December 2008
Online at stacks.iop.org/JPhysCM/21/015401

**Abstract**

The structural and physical properties of the recently discovered electronic ferroelectric materials $LuFe_2O_4$ and $Lu_2Fe_3O_7$ have been investigated for Mg substitution of Fe. X-ray diffraction data demonstrate that the lattice parameters in both systems change progressively with increasing Mg content, with a smaller unit cell volume on replacing $Fe^{2+}$ by $Mg^{2+}$. X-ray absorption near-edge spectroscopy experiments at the Fe K-edge show that the average Fe oxidation state is slightly increased along with Mg doping in $Lu_2Fe_3O_7$ materials, consistent with isomorphous replacement of $Fe^{2+}$ by $Mg^{2+}$. Measurements of dielectric properties demonstrate that Mg doping could have an effect on the electron hopping energy between $Fe^{2+}$ and $Fe^{3+}$ ions. Transmission electron microscopy and magnetization analysis reveal that Mg doping in $LuFe_2O_4$ has a much greater influence than in $Lu_2Fe_3O_7$ on both the charge ordering and the low-temperature magnetic properties.

(Some figures in this article are in colour only in the electronic version)

## 1. Introduction

Multiferroic materials have stimulated considerable interest because of their remarkable properties that could yield immense benefits in advanced materials for technical applications in modern electronic devices such as memory elements, filtering and switching devices [1]. Electronic ferroelectricity from charge ordering (CO) is currently a significant issue that has been extensively investigated in the charge/spin frustrated $LuFe_2O_4$ system; moreover, a giant magneto-dielectric response was observed in this material at room temperature [2–6]. $LuFe_2O_4$ consists of two layers: a hexagonal double layer of Fe ions (W layer), with an average valence of $Fe^{2.5+}$, which is sandwiched by a thick Lu–O layer [5, 6]. The spin or charge behavior in the W layers directly affects the magnetic features and also the ferroelectricity [6]. Systematic TEM analysis demonstrates that the charges in the W layers at low temperatures are well crystallized in a charge-stripe phase, in which the charge-density wave behavior in a nonsinusoidal fashion results in elemental electric dipoles for ferroelectricity [7].

For technological applications to be viable, large improvements are needed in both the sensitivity and stability of these new materials. Chemical substitution and structural layer intercalation have been considered as potentially effective approaches; our previous experimental investigations in the layered series of $LuFe_2O_4(LuFeO_3)_n$ ($n = 0$, 1 and 2) reveal that the $(RFeO_3)$-layer intercalation results in notable changes in dielectric and magnetic properties and CO features [8].

Structurally, each layered $LuFe_2O_4(LuFeO_3)_n$ phase is simply constructed by an alternate stacking of $LuFe_2O_4$ and $(LuFeO_3)_n$ blocks along the $c$-axis direction [9]. Schematic structures of the layered family are shown in figure 1 for $n = 0$ and 1. It can be seen that both $n = 0$ and 1 phases contain charge frustrated $Fe_2O_{2.5}$ layers (W layers), while the $n = 1$ phase also contains $FeO_{1.5}$ layers (V layers). The equal numbers of $Fe^{2+}$ and $Fe^{3+}$ in a W layer can be ordered and result in electronic ferroelectricity as extensively discussed in

[4] Author to whom any correspondence should be addressed.

 

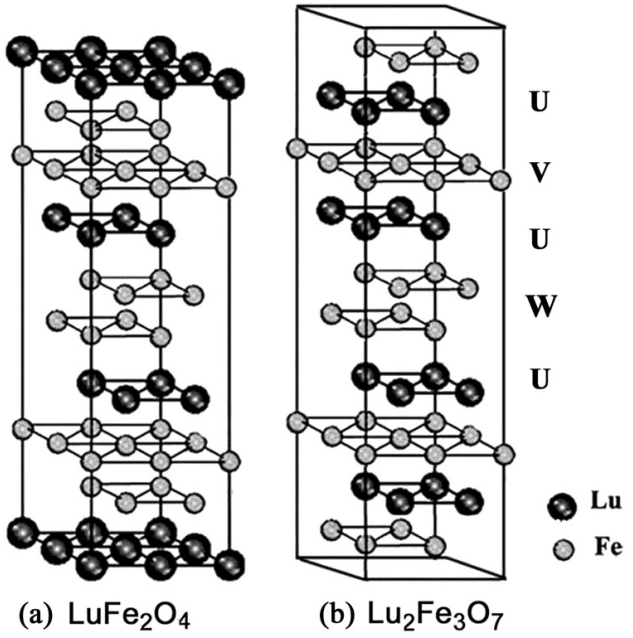


**Figure 1.** Structural models schematically illustrating the Lu–O layer, Fe–O double- and single-layer stacking alternately along the $c$ axis for the $LuFe_2O_4(LuFeO_3)_n$ phase (a) $n = 0$ and (b) $n = 1$; O-atoms are omitted for clarity.

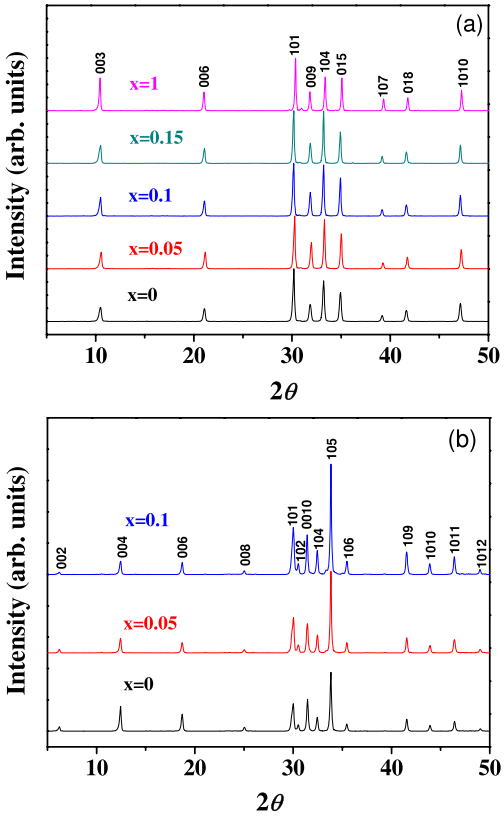


**Figure 2.** The XRD patterns for (a) $LuFeFe_{(1-x)}Mg_xO_4$ ($x = 0$, 0.05, 0.10, 0.15 and 1) and (b) $Lu_2Fe_2Fe_{(1-x)}Mg_xO_7$ ($x = 0$, 0.05 and 0.10) samples.

the context of the $LuFe_2O_4$ ($n = 0$) phase [7]. The valence states of Fe ions in the $Lu_2Fe_3O_7$ ($n = 1$) are much more complex: the valence state for Fe is ideally, on average, 2.67, assuming stoichiometric oxygen content. The measurements of the Mössbauer spectrum suggested that the Fe ions in the V layer have a valence state of $Fe^{3+}$ and therefore CO probably occurs in the W layers [10]. However, our recent study on $Lu_2Fe_3O_7$ revealed that charge disproportionation also appears in the V layers recognizable as clear CO modulations, suggesting that the intercalation of $LuFeO_3$ blocks could yield notable effects on the interaction among layers and cause further charge redistribution on the Fe sites [8].

Chemical substitution usually has a strong influence on both charge ordering and low-temperature magnetic properties for charge ordered compounds [11] and has been considered as an effective way to tune the dielectric and ferroelectric properties for ferroelectric systems [12]. For layered $LuFe_2O_4(LuFeO_3)_n$ phases, substitution of other ions for Fe within the Fe–O layers is therefore a significant way to understand the correlation between the physical properties and charge ordered states.

It is known that the nonmagnetic $Mg^{2+}$ can replace $Fe^{2+}$ (the two ions have similar radii) in $LuFe_2O_4$ to form $LuFeMgO_4$, which is an antiferromagnet with magnetic transition temperature at about 33 K [13, 14]. In this paper, we have performed an extensive investigation on the Mg-doped materials with nominal compositions of $LuFeFe_{(1-x)}Mg_xO_4$ and $Lu_2Fe_2Fe_{(1-x)}Mg_xO_7$, in which the charge/spin ordering within the doubled Fe layers is expected to be altered. The experimental results showed that doping by Mg greatly affects the structural and physical properties; certain materials show remarkable changes of magnetic properties and dielectric features in comparison with those observed in the parent $LuFe_2O_4$ and $Lu_2Fe_3O_7$ materials.

## 2. Experiment

Polycrystalline samples of $LuFeFe_{(1-x)}Mg_xO_4$ ($x = 0$, 0.05, 0.10 and 0.15) and $Lu_2Fe_2Fe_{(1-x)}Mg_xO_7$ ($x = 0$, 0.05 and 0.10) were synthesized by conventional solid-state reactions as reported in [15]. A stoichiometric amount of $Lu_2O_3$ (99.99%), guaranteed reagent grade $Fe_2O_3$ and MgO (99.95%) were fully mixed in an agate mortar. After that, the raw materials were pressed into pellets and sintered in an atmosphere having an oxygen partial pressure controlled by using the mixed gas $CO_2/H_2$ at 1200 °C for 72 h. $LuFeMgO_4$ ($LuFeFe_{(1-x)}Mg_xO_4$ with $x = 1$) was synthesized via a similar solid-state reaction procedure with air as flowing gas following the literature [16]. Structural and phase purity characterizations were carried out by powder x-ray diffraction (XRD) using a Rigaku diffractometer with Cu K$\alpha$ radiation. Transmission electron microscopy (TEM) investigations were performed on a Tecnai F20 (200 kV) electron microscope. TEM samples were prepared by mechanical polishing, dimpling and ion milling. Magnetization measurements between 5 and 300 K were carried out on a commercial superconductor quantum interference device magnetometer. The zero-field-cooling (ZFC) and field-cooling (FC) curves were obtained at applied fields of 100 Oe. The dielectric constant as a function of

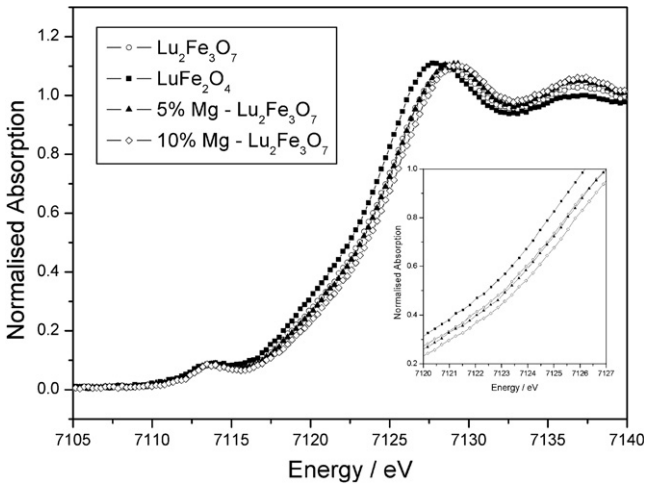


**Figure 3.** The Fe K-edge XANES spectrum of $Lu_2Fe_3O_7$, $LuFe_2O_4$ and $Lu_2Fe_2Fe_{(1-x)}Mg_xO_7$ with $x = 0.05$ and 0.10. The inset shows the edge region.

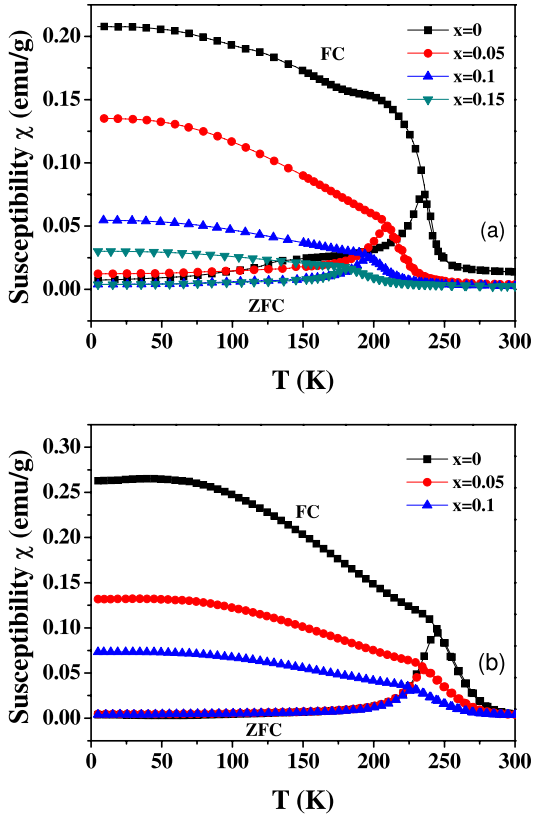


**Figure 4.** The ZFC and FC magnetization of (a) $LuFeFe_{(1-x)}Mg_xO_4$ ($x = 0$, 0.05, 0.10 and 0.15) and (b) $Lu_2Fe_2Fe_{(1-x)}Mg_xO_7$ ($x = 0$, 0.05 and 0.10) as a function of temperature at an applied magnetic field of 100 Oe. (Part of the data in (a) is taken from figure 11(b) of [20].)

temperature was measured using the LCR METER ZM2353 under different frequencies from 10 to 200 kHz.

XANES (x-ray absorption near-edge structure) experiments were performed on Station 9.3 of the Daresbury Synchrotron Radiation Source (SRS), UK at the Fe K-edge. The SRS operates at 2 GeV with an average stored current of 2 mA.

**Table 1.** Lattice parameters $a$, $c$ and unit cell volume of $Lu_2Fe_2Fe_{(1-x)}Mg_xO_7$ ($x = 0$, 0.05 and 0.10) and $LuFeFe_{(1-x)}Mg_xO_4$ ($x = 0$, 0.05, 0.10, 0.15 and 1) samples.

| Samples | $a$ (Å) | $c$ (Å) | Unit cell volume (Å$^3$) |
|---|---|---|---|
| $Lu_2Fe_3O_7$ | 3.4543(7) | 28.4246(9) | 293.7407(2) |
| $Lu_2Fe_2Fe_{0.95}Mg_{0.05}O_7$ | 3.4523(2) | 28.4311(0) | 293.4583(3) |
| $Lu_2Fe_2Fe_{0.9}Mg_{0.1}O_7$ | 3.4516(8) | 28.4397(7) | 293.4389(0) |
| $LuFe_2O_4$ | 3.4404(5) | 25.2531(7) | 258.8677(0) |
| $LuFe_{1.95}Mg_{0.05}O_4$ | 3.4400(7) | 25.2455(0) | 258.7309(5) |
| $LuFe_{1.9}Mg_{0.1}O_4$ | 3.4400(6) | 25.2419(3) | 258.6928(4) |
| $LuFe_{1.85}Mg_{0.15}O_4$ | 3.4394(0) | 25.2405(2) | 258.5796(7) |
| $LuFeMgO_4$ | 3.4134(4) | 25.1907(5) | 254.1889(0) |

In our experiments the incident x-ray energy was selected using an Si(220) double-crystal monochromator and data measured in transmission mode from samples of solid diluted with polyethylene powder and pressed into ∼1 mm thick pellets. In order to calibrate the XANES spectrum, data were simultaneously recorded from an Fe foil placed between the transmission and a monitor ion chamber. The spectra were recorded with a step equivalent to the energy of a minimum step of 0.3 eV (close to the estimated instrumental resolution of ∼0.5 eV), and were calibrated and normalized using the programs EXCALIB and EXBROOK [17] to produce XANES spectra normalized to the pre-edge and edge step, determined by fitting polynomials to the raw data.

## 3. Results and discussion

### *3.1. Powder x-ray diffraction data analysis*

We have successfully synthesized Mg-doped $LuFe_2O_4$ and $Lu_2Fe_3O_7$ samples with nominal compositions of $LuFeFe_{(1-x)}Mg_xO_4$ ($x = 0$, 0.05, 0.10, 0.15 and 1) and $Lu_2Fe_2Fe_{(1-x)}Mg_xO_7$ ($x = 0$, 0.05 and 0.10). The powder x-ray diffraction patterns taken from the $Lu_2Fe_2Fe_{(1-x)}Mg_xO_7$ ($x \leqslant 0.10$) and $LuFeFe_{(1-x)}Mg_xO_4$ ($x \leqslant 0.15$, $x = 1$) samples can be confidently indexed using hexagonal cells with the $P6_3/mmc$ space group and $R\bar{3}m$ space group, respectively, and no peaks from impurity phases are observed. Figures 2(a) and (b) show the XRD patterns taken from Mg-doped $LuFe_2O_4$ and $Lu_2Fe_3O_7$ samples at room temperature. Table 1 lists the structural parameters and unit cell volume obtained from XRD experiments. It is clear that the lattice parameters change systematically with the doping level ($x$) in both systems. The Mg-doped samples have smaller unit cell volumes than the parent materials, expected with the slightly smaller radius of $Mg^{2+}$ compared with $Fe^{2+}$. This fact demonstrates that the expected substitution within Fe–O sheets has been successfully carried out in these samples.

### *3.2. X-ray absorption near-edge spectroscopy measurements*

The successful substitution of Mg within Fe–O sheets has been further confirmed by the x-ray absorption near-edge spectroscopy (XANES) study for $Lu_2Fe_2Fe_{(1-x)}Mg_xO_7$ ($x = 0$, 0.05 and 0.10). The metal oxidation state is well known to

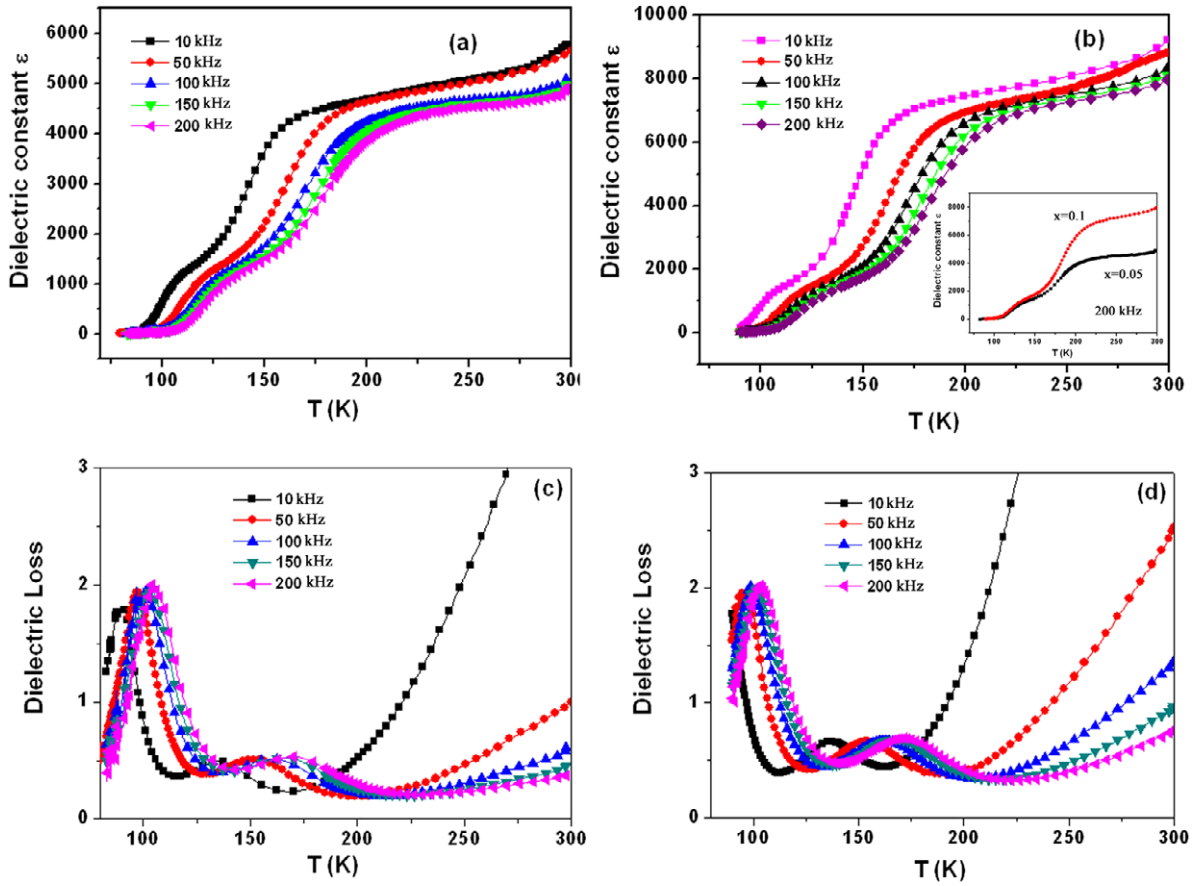


**Figure 5.** The dielectric constant for (a) $x = 0.05$ and (b) $x = 0.10$ and the dielectric loss for (c) $x = 0.05$ and (d) $x = 0.10$ of $Lu_2Fe_2Fe_{(1-x)}Mg_xO_7$ samples as a function of temperature at different frequencies.

cause a shift of the absorption edge in the XANES spectrum: for higher oxidation states with stronger bonds, the split of atomic orbitals is larger, the energy of anti-bond orbitals is higher and the absorption edge shifts to higher energy. For our samples, i.e. $Lu_2Fe_3O_7$, $LuFe_2O_4$ and $Lu_2Fe_2Fe_{(1-x)}Mg_xO_7$ with $x = 0.05$ and 0.10, shown in figure 3, $LuFe_2O_4$ has the lowest energy edge shift, since it has Fe in the lowest oxidation state (+2.5 on average), followed by $Lu_2Fe_3O_7$ (+2.67 on average). When a Mg atom is doped on an Fe atom site, the average oxidation state of the remaining Fe is higher, and we observe a small, but real shift to higher energy. Our XANES results are therefore consistent with the replacement of $Fe^{2+}$ by $Mg^{2+}$ in an isomorphous manner with retention of oxygen stoichiometry in $Lu_2Fe_3O_7$.

### *3.3. Magnetization measurements*

Measurements of magnetization on the samples revealed that Mg doping influences the temperature of phase transitions and magnetic properties. Figures 4(a) and (b) show the ZFC and FC magnetizations of $LuFeFe_{(1-x)}Mg_xO_4$ ($x = 0$, 0.05, 0.10 and 0.15) and $Lu_2Fe_2Fe_{(1-x)}Mg_xO_7$ ($x = 0$, 0.05 and 0.10) as a function of temperature at an applied field of 100 Oe. Results obtained from all samples show clear cusp-like peaks in the ZFC curves; similar field-cooling effects are also observed. It is also visible that the magnetic ordering transition decreases remarkably with doping content in both systems, i.e. from about 235 K in $LuFe_2O_4$ to a temperature of about 180 K in $LuFe_{1.85}Mg_{0.15}O_4$ and from about 245 K in $Lu_2Fe_3O_7$ to a lower temperature of about 230 K in $Lu_2Fe_2Fe_{0.9}Mg_{0.1}O_7$. The strong exchange frustration in the double Fe layers could be partially released when a triangular antiferromagnet is diluted with a nonmagnetic ion such as $Mg^{2+}$. $LuFeMgO_4$ has been reported to be the simplest model diluted antiferromagnet with strong geometrical frustration [13, 14], where its magnetic transition temperature is about 33 K. Another feature revealed in figure 4 is that the magnetization becomes weaker in both FC and ZFC curves (especially the FC curves) as more magnetic $Fe^{2+}$ ions are substituted by nonmagnetic $Mg^{2+}$ ions, i.e. the highest values of FC curves for $Lu_2Fe_2Fe_{(1-x)}Mg_xO_7$ with $x = 0$, 0.05 and 0.10 are 0.26 emu $g^{-1}$, 0.13 emu $g^{-1}$ and 0.07 emu $g^{-1}$, respectively, under the applied field of 100 Oe in the measured temperature range (figure 4(b)).

Previous investigations on the magnetic properties of $LuFe_2O_4$ and $Lu_2Fe_3O_7$ materials suggest that the characteristic peak at about 200 K is due to the spin order in the W layer, while those in the V layer seem to be paramagnetic down to 80 K [18]. Detailed analysis also suggests that, with the same Mg doping value in the W layer, the magnetic ordering transition temperature at about 200 K decreases much faster for $LuFe_2O_4$ material in comparison with $Lu_2Fe_3O_7$. When the doping level is 10% ($x = 0.1$),

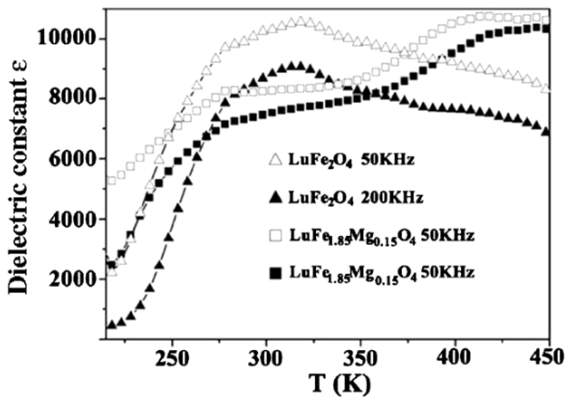


**Figure 6.** The dielectric constant of $LuFe_2O_4$ and $LuFe_{1.85}Mg_{0.15}O_4$ as a function of temperature, measured at frequencies of 50 and 200 kHz. (Figure reprinted with permission from [20]. Copyright (2007) by the American Physical Society.)

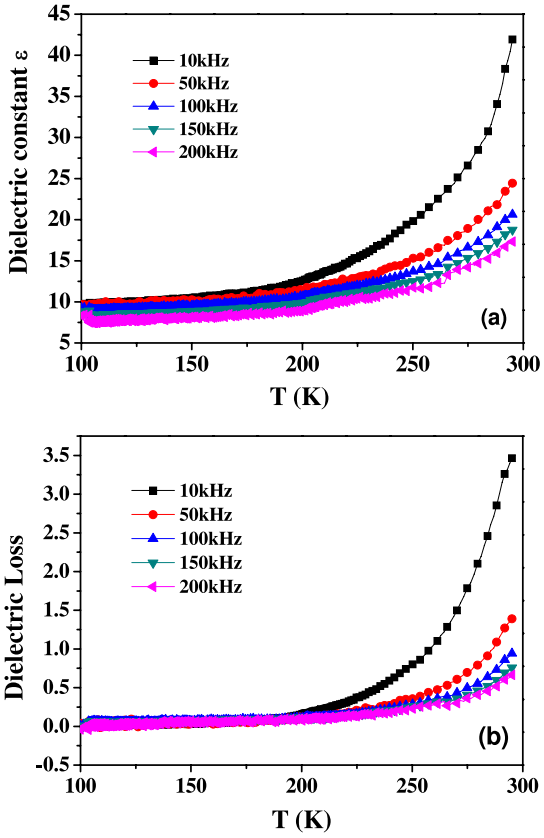


**Figure 7.** (a) The dielectric constant and (b) the dielectric loss of $LuFeMgO_4$ samples as a function of temperature at different frequencies.

for example, the transition temperature shift for the $Lu_2Fe_3O_7$ system is 15 K, while it is 40 K for the $LuFe_2O_4$ system. We therefore conclude that intercalation of $LuFeO_3$ blocks could yield notable effects on the interaction among layers and cause further charge redistribution on the Fe sites [8]. Actually our previous HRTEM result has confirmed that the charge disproportionation also appears in the V layers recognizable as clear CO modulations in $Lu_2Fe_3O_7$ [8]. We could expect that Mg substitution in V layers reduces the actual doping content in W layers; therefore, the magnetic ordering transition temperature decreases much slower for $Lu_2Fe_3O_7$ compared with $LuFe_2O_4$ material.

### *3.4. Dielectric properties*

It is commonly noted that $LuFe_2O_4$ material has a large dielectric constant ranging from 6000 to 10 000 at room temperature [5]; thus this material could possibly play an important role in the development of novel electric and electronic devices.

Our previous work showed that $LuFeO_3$-block intercalation is one efficient way to tune the dielectric property in this system [8]. The dielectric data of $Lu_2Fe_3O_7$ are comparable with results obtained from $LuFe_2O_4$, but the temperature (and also frequency) dependence of the dielectric data has a notable difference [8]. Here, we will discuss the Mg doping effect on the dielectric property in both systems.

Figure 5 shows the temperature dependence (during heating) of the dielectric constant and loss factor of the Mg-doped $Lu_2Fe_2Fe_{(1-x)}Mg_xO_7$ with $x = 0.05$ and 0.10. The remarkable features in the $\varepsilon$–$T$ curves are that there are two evident step-wise anomalies and they both show strong frequency dispersion. The low-temperature anomaly as shown in figure 5(a) is located at 86 K at 10 kHz, and shifts to higher temperature with increasing frequencies, e.g. 110 K at 200 kHz. Meanwhile, dielectric loss peaks are detected at the corresponding critical temperatures. This behavior is similar to that of dielectric relaxation caused by electronic ferroelectricity as observed in $LuFe_2O_4$ [5]. In both samples, the dielectric constant is small at lower temperatures, and then it increases rapidly up to almost the same level: after that, it continues to increase but much more slowly before increasing again rapidly with increasing temperature and reaching a plateau at about 200 K. At this stage the two samples show huge differences. For all the measuring frequencies, the dielectric constant increases much faster in $Lu_2Fe_2Fe_{(1-x)}Mg_xO_7$ with $x = 0.10$. The value of the second plateau is almost double the dielectric constant of $Lu_2Fe_2Fe_{(1-x)}Mg_xO_7$ with $x = 0.05$, as shown in the inset of figure 5(b), which compares the two $\varepsilon$–$T$ curves with the frequency of 200 kHz.

Figure 6 shows the dielectric constant of $LuFe_{1.85}Mg_{0.15}O_4$ as a function of temperature in comparison with the data of $LuFe_2O_4$. The curves also show two plateau-like features with distinctive dispersion but at much higher temperatures in comparison with $Lu_2Fe_3O_7$. It is easily seen that substitution of $Mg^{2+}$ for $Fe^{2+}$ also clearly increases the value of the dielectric constant at the second plateau.

Figure 7(a) shows the temperature dependence of the real parts of the dielectric constant of $LuFeMgO_4$; the dielectric constant of $LuFeMgO_4$ is two orders of magnitude smaller than $LuFe_2O_4$ and the dielectric constant increases continually during the whole measured temperature range and no anomaly was observed. Meanwhile, there are no dielectric loss peaks detected in the corresponding $\delta$–$T$ curves as shown in figure 7(b). Our dielectric data on $LuFeMgO_4$ further support that the charge frustration and CO occurring at low

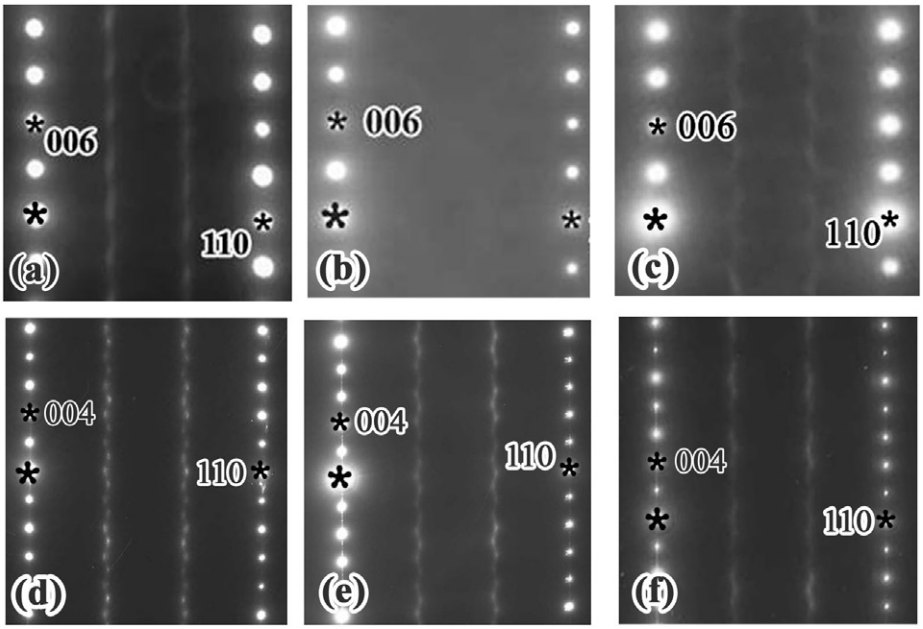


**Figure 8.** Electron diffraction patterns of (a) $LuFe_2O_4$ and (b) $LuFeFe_{0.85}Mg_{0.15}O_4$ along $[1\bar{1}0]$ zone-axis directions at room temperature. Electron diffraction patterns of (c) $LuFeFe_{0.85}Mg_{0.15}O_4$ along $[1\bar{1}0]$ zone-axis directions at 100 K. Electron diffraction patterns of (d) $Lu_2Fe_3O_7$, (e) $Lu_2Fe_2Fe_{0.95}Mg_{0.05}O_7$ and (f) $Lu_2Fe_2Fe_{0.90}Mg_{0.10}O_7$ along $[1\bar{1}0]$ zone-axis directions at room temperature.

temperatures is the origin of the unusual dielectric property in $LuFe_2O_4$.

Yamada *et al* proposed a model to explain the two dielectric dispersions in $LuFe_2O_4$ [5, 19]. According to the model, the high-temperature dispersion originates from the electron hopping between Fe ions on the disordered sites, whose charge is not definite but fluctuating between 2+ and 3+ states, while the low-temperature dispersion is related to the motion of the discommensuration boundaries, whose elementary process is also electron hopping between $Fe^{2+}$ and $Fe^{3+}$ ions [5, 19].

Mg isomorphous substitution could have an effect on the electron hopping energy between $Fe^{2+}$ and $Fe^{3+}$ ions, as well as the nature of the polar domain boundaries. The significant enhancement of the dielectric constant at the high-temperature dispersion could be caused by the combination of these two aspects.

### *3.5. TEM study on charge ordering*

In order to fully understand the Mg doping effect on the charge ordering and microstructure features of the $LuFe_2O_4$ and $Lu_2Fe_3O_7$ materials, we have performed a series of investigations by means of selected-area electron diffraction.

Figures 8(a) and (b) show the electron diffraction patterns of $LuFeFe_{(1-x)}Mg_xO_4$ with $x = 0$ and 0.15 along the $[1\bar{1}0]$ zone-axis directions at room temperature. Figure 8(a) reveals the superstructure reflections as diffuse streaks on ($h = 3$, $h = 3$, $l$) lines along the $c$ direction. The superstructure reflections contain notable contributions from the CO twinning, which often results in a zigzag type of superstructure streaks as noted in previous publications [20]. It is very clear that the intensities of the superstructure reflections decrease progressively with increasing Mg content, and almost vanish at the $x = 0.15$ sample, suggesting the charge ordered states are suppressed due to Mg doping at room temperature. Further *in situ* TEM cooling experiments show that the superstructure caused by charge ordering appears again when the temperature is lower than 250 K: figure 8(c) gives an SAED pattern taken along the $[1\bar{1}0]$ zone-axis direction of an $x = 0.15$ sample at 100 K.

Figures 8(d)–(f) show the electron diffraction patterns of $Lu_2Fe_2Fe_{(1-x)}Mg_xO_7$ with $x = 0$, 0.05 and 0.10 along the $[1\bar{1}0]$ zone-axis direction at room temperature. As we previously reported [8], the $Lu_2Fe_3O_7$ shows remarkable multiferroic properties in correlation with the essential CO nature existing in this kind of material. The charge ordered state in the samples can be characterized by two incommensurate modulations [8], which is much more complex than that in $LuFe_2O_4$. In contrast with the diffuse satellite streaks in $LuFe_2O_4$ at room temperature, $Lu_2Fe_3O_7$ often gives rise to sharp superlattice spots, suggesting a longer CO coherence length, which would favor the existence of larger ferroelectric domains in the present material [8]. It is very clear that the intensities of the superstructure reflections decrease progressively with increasing Mg content. Further analysis of the data also demonstrates that Mg doping in $LuFe_2O_4$ has a more evident effect on charge ordering than in $Lu_2Fe_3O_7$; this result is consistent with the magnetic data.

## 4. Conclusions

In summary, we have successfully synthesized polycrystalline samples of $LuFeFe_{(1-x)}Mg_xO_4$ ($x = 0$, 0.05, 0.10, 0.15 and 1) and $Lu_2Fe_2Fe_{(1-x)}Mg_xO_7$ ($x = 0$, 0.05 and 0.10). Their structure and low-temperature physical properties have been investigated and analyzed as a function of increasing

doping level. Our investigations demonstrate that the lattice parameters in both systems change progressively with increasing Mg content, with a smaller unit cell volume on replacing $Fe^{2+}$ by $Mg^{2+}$ and the average Fe oxidation state is slightly increased along with Mg doping in $Lu_2Fe_3O_7$, consistent with isomorphous replacement of $Fe^{2+}$ by $Mg^{2+}$. The charge ordering and magnetic phase transition at about 200 K are suppressed by Mg doping in both systems; the dielectric constants in $LuFe_2O_4$ and $Lu_2Fe_3O_7$ are evidently influenced by the Fe-site doping. It is also noted that the Mg doping in $LuFe_2O_4$ has a visibly stronger influence than Mg doping in $Lu_2Fe_3O_7$ on both charge ordering and low-temperature magnetic properties. This difference is possibly attributable to charge disproportionation appearing in both the W and V layers, rather than in just the W layer as previously suggested [18].

## Acknowledgments

We would like to thank Y Li for her help during TEM sample preparation. This work is supported by the National Science Foundation of China, the Knowledge Innovation Project of the Chinese Academy of Sciences, and the 973 projects of the Ministry of Science and Technology of China. We thank the STFC (UK) for the provision of beamtime at the SRS.

## References

[1] Spaldin N A and Fiebig M 2005 *Science* **309** 391
[2] Ikeda N, Kohn K, Kito H, Akimitsu J and Siratori K 1995 *J. Phys. Soc. Japan* **64** 1371
[3] Ikeda N, Yamada Y, Nohdo S, Inami T and Katano S 1998 *Physica* B **241–243** 820
[4] Subramanian M A, He T, Chen J Z, Rogado N S, Calvarese T G and Sleight A W 2006 *Adv. Mater.* **18** 1737
[5] Ikeda N, Kohn K, Myouga N, Takahashi E, Kitoh H and Takeawa S 2000 *J. Phys. Soc. Japan* **69** 1526
[6] Yamada Y, Kitsuda K, Nohdo S and Ikeda N 2000 *Phys. Rev.* B **62** 12167
[7] Zhang Y, Yang H X, Ma C, Tian H F and Li J Q 2007 *Phys. Rev. Lett.* **98** 247602
[8] Yang H X, Zhang Y, Ma C, Tian H F, Qin Y B, Zhao Y G and Li J Q 2008 arXiv:0803.0819v2
[9] Kato K, Kawada I, Kimizuka N, Shindo I and Katsura T 1976 *Z. Kristallogr.* **143** 278
[10] Tanaka M, Kimizuka N, Akimitsu J, Funahashi S and Siratori K 1983 *J. Magn. Magn. Mater.* **31–34** 769
[11] Shi Y G, Yang H X, Liu X, Ma W J, Nie C J, Huang W W and Li J Q 2005 *Physica* C **299–305** 432
[12] Yu B F, Li M Y, Liu J, Guo D Y, Pei L and Zhao X Z 2008 *J. Phys. D: Appl. Phys.* **41** 065003
[13] Tanaka M, Himoto E and Todate Y 1995 *J. Phys. Soc. Japan* **64** 2621
[14] Todate Y, Himoto E, Kikuta C, Tanaka M and Suzuki J 1998 *Phys. Rev.* B **57** 485
[15] Kimizuka N, Takenaka A, Sasada Y and Katsura T 1974 *Solid State Commun.* **15** 1199
[16] Kimizuka N and Takayama E 1981 *J. Solid State Chem.* **40** 109
[17] Binsted N, Campbell J W, Gurman S J and Stephenson P C 1991 *EXAFS Data Analysis Program* Daresbury Laboratory
[18] Iida J, Tanaka M and Funahashi S 1992 *J. Magn. Magn. Mater.* **104–107** 827
[19] Takahashi E and Kohn K 1998 *J. Korean Phys. Soc.* **32** S44
[20] Zhang Y, Yang H X, Guo Y Q, Ma C, Tian H F, Luo J L and Li J Q 2007 *Phys. Rev.* B **76** 184105